PCCP

Dynamic Article Links

Cite this: *Phys. Chem. Chem. Phys.*, 2011, **13**, 13565–13571

www.rsc.org/pccp

PAPER

Growth of sputter-deposited gold nanoparticles in ionic liquids

Evert Vanecht,[a] Koen Binnemans,*[a] Jin Won Seo,[b] Linda Stappers[b] and Jan Fransaer[b]

Received 28th February 2011, Accepted 24th May 2011
DOI: 10.1039/c1cp20552h

The growth of gold nanoparticles (NPs) synthesized by sputter deposition on an ionic liquid surface is studied *in situ* in the bulk phase of the ionic liquids (ILs) 1-butyl-3-methylimidazolium dicyanamide $[C_1C_4Im][N(CN)_2]$, 1-butyl-3-methylimidazolium bis(trifluoromethanesulfonyl)amide $[C_1C_4Im][Tf_2N]$, 1-butyl-3-methylimidazolium tetrafluoroborate $[C_1C_4Im][BF_4]$, 1-butyl-3-methylimidazolium hexafluorophosphate $[C_1C_4Im][PF_6]$ and 1-butyl-3-methylimidazolium triflate $[C_1C_4Im][TfO]$. It is found that primary nanoparticles with a diameter smaller than 2.5 nm are present in the sample immediately after sputtering. Growth of these primary particles proceeds after the end of the sputtering process and stops when the nanoparticles reach a certain size. Depending on the viscosity of the ionic liquid this growth process can proceed several hours to several days. The growth speed is fastest for the least viscous ionic liquid and follows the trend $[C_1C_4Im][N(CN)_2] > [C_1C_4Im][Tf_2N] > [C_1C_4Im][TfO] > [C_1C_4Im][BF_4] > [C_1C_4Im][PF_6]$. It is also found that a higher concentration of sputtered gold results in faster growth of the gold nanoparticles. A discussion on the growth mechanism of sputtered gold NPs is included.

Introduction

The synthesis of metal nanoparticles in ionic liquids (ILs) is a very active field of research.[1] Novel synthesis methods take advantage of the extremely low vapor pressure of ionic liquids, so that the preparation of nanoparticles can be performed at low pressure or even under high vacuum conditions.[15] Endres, Janek and coworkers prepared copper, silver and palladium nanoparticles by glow discharge electrodeposition.[2] A recent paper described the formation of gold nanoparticles by reduction of gold(III) ions by the electron beam of a scanning electron microscope.[3] Based on the work of Wagener and Günther,[25] Torimoto and coworkers reported on a method for the synthesis of gold nanoparticles by *sputter deposition*.[4] Gold atoms were knocked out from a gold target cathode by the argon ions in an argon plasma and were sputtered on an ionic liquid surface. This sputter deposition is a very clean synthesis method, because it does not introduce other chemicals, such as metal precursors or reducing and stabilizing agents, which can have a considerable influence on the suspension and its future application (*e.g.* stability, catalysis). The nanoparticles prepared by this method were found to be very stable, even in the absence of additional stabilizing agents. In addition, it has also been shown that bimetallic alloy nanoparticles can be obtained by using a segmented gold–silver target,[5] or by sputtering silver nanoparticles into an ionic liquid containing dissolved $HAuCl_4$.[6]

The stability of metal nanoparticles in ionic liquids has been vividly debated, but few literature data exist on the growth of metal nanoparticles in ionic liquids. The growth mechanisms of metal nanoparticles are currently poorly understood. Janiak and co-workers recently published a "stop-and-go, ligand-free nucleation and growth" mechanism of gold NPs in ionic liquids.[8] It suggested that small primary clusters (1–3 nm) grow by colliding and coalescing to form crystalline gold NPs. They describe that ILs do not act as capping ligands, but as a kinetically stabilizing, dynamic molecular network in which the gold atoms and clusters move by diffusion and cluster together. In a sputter deposition study using different 1-alkyl-3-methylimidazolium tetrafluoroborate ionic liquids, it was proposed that the initial aggregation of gold atoms and clusters to nanoparticles takes place on the surface of the ionic liquid and that the surface tension of the ionic liquid influences the initial formation process of gold nanoparticles on the ionic liquid surface.[7] This study also revealed that the viscosity affected the aggregation process towards larger nanoparticles during the dispersion of the gold nanoparticles from the surface into the bulk ionic liquid. Dupont and co-workers argued that both nucleation and growth occur on the IL surface after sputtering and that viscosity nor surface tension but surface composition affects the growth of the metal nanoparticles.[19]

[a] *Katholieke Universiteit Leuven, Department of Chemistry, Celestijnenlaan 200F-P.O. Box 2404, B-3001 Heverlee, Belgium. E-mail: Koen.Binnemans@chem.kuleuven.be; Fax: +32 16327992; Tel: +32 16727446*
[b] *Katholieke Universiteit Leuven, Department of Metallurgy and Materials Engineering (MTM), Kasteelpark Arenberg 44-P.O. Box 2450, B-3001 Heverlee, Belgium*

As part of a research program on the synthesis and properties of nanoparticles in ionic liquids, we investigated the influence of the ionic liquid composition on the size and size distribution of gold nanoparticles prepared by sputter deposition. Our initial experiments were found very difficult to reproduce: experiments under the same sputtering conditions and using the same ionic liquid gave different size distributions after analysis of the transmission electron microscopy (TEM) pictures. This experimental failure was initially attributed to difficulties associated with the sample preparation for TEM measurements. It was also noticed that the UV-VIS absorption spectra of some samples showed a sharp surface plasmon resonance (SPR) band at about 520 nm, whereas in other samples this absorption band was much broader or even absent. The striking observation that the SPR band changed as a function of time after sputtering suggested us to perform experiments under time-controlled conditions.

This paper reports on the preparation of gold nanoparticles by sputter deposition on an ionic liquid and on the growth of these nanoparticles in the bulk phase of the ionic liquid after the end of the sputtering process. Imidazolium ionic liquids with different anions have been used for a systematic study of the growth process of sputtered nanoparticles in ionic liquids.

Experimental

The ionic liquids 1-butyl-3-methylimidazolium dicyanamide $[C_1C_4Im][N(CN)_2]$ (>98%), 1-butyl-3-methylimidazolium bis(trifluoromethanesulfonyl)amide $[C_1C_4Im][Tf_2N]$ (99%), 1-butyl-3-methylimidazolium tetrafluoroborate $[C_1C_4Im][BF_4]$ (99%) and 1-butyl-3-methylimidazolium triflate $[C_1C_4Im][TfO]$ (99%) were purchased from IoLiTec. They were dried at a *Schlenk* line (2×10^{-3} mbar), first at 45 °C for 3 h and then for 2 h at 80 °C under stirring. The flasks were filled with argon and kept in a glove-box with a water content below 2 ppm. Coulometric Karl Fischer titrations showed that the water content of the dried ionic liquids was less than 30 ppm.

The sputter experiments were performed using a Bal-Tec SCD 005 sputter coater. The sputter coater apparatus was placed in a glove-box (<2 ppm water). This was done to keep the ionic liquids completely dry during manipulations before and after sputtering. A gold foil (99.99%) of 5.4 cm diameter and a thickness of 0.2 mm was used as a target. An argon pressure of 0.1 mbar, an electric current of 50 mA, a sputter time of 60 s and a target–substrate distance of 40 mm were applied unless otherwise specified. A PTFE container (30 mm diameter and 5 mm deep) containing an aliquot of ionic liquid (4 mL) was placed on the sputter table in the vacuum chamber of the sputter coater.

UV-VIS absorption spectra were recorded between 800 and 300 nm at room temperature on a Cary Varian 5000 spectrophotometer. For the spectroscopic measurements, the ionic liquid containing the nanoparticles was poured into a quartz cuvette with an optical path length of 10 mm.

Transmission electron microscopy (TEM) and high-resolution TEM pictures were taken on a Philips CM 200 FEG apparatus operating at an acceleration voltage of 200 kV. The nanoparticles were studied by TEM directly in the ionic liquid. The TEM samples were prepared by dipping a copper grid (300 mesh) covered with a lacey carbon film (from Agar Scientific) into the ionic liquid solution and draining the excess of ionic liquid with a paper tissue. The size distribution of gold nanoparticles was determined by measuring the size in TEM images (more than 300 particles for each sample).

The water content of the ionic liquids was determined with a Mettler Toledo DL 39 Karl Fischer Coulometer. The viscosity of the ionic liquids was determined with a Brookfield DV-II+Pro Cone/plate set-up viscometer at a temperature of 298 K.

Gold concentration in the ionic liquids was determined with a Total Reflection X-Ray Fluorescence (TXRF) spectrometer S2 Picofox (Bruker AXS). Copper was used as an internal standard. A 50 : 50 vol% mixture of acetone and water was added to 1 g of the sputtered ionic liquid to reach a volume of 20 mL. 10 μL of a 1000 ppm Cu aqueous solution was added as an internal standard to 990 μL of the IL/Au/acetone/water suspension. After mixing, 10 μL of this solution was transferred onto a TXRF quartz glass sample holder and dried in an oven at 80 °C.

The amount of sputtered gold during sputter deposition was monitored by a Balzers QSG 301 Quartz Crystal Microbalance (QCMB) that was placed inside the vacuum sputter chamber.

Gold extraction from the sputtered ionic liquid was done with a sodium cyanide solution (10^{-1} M). The pH was kept at 12 by adding NaOH to prevent the formation of HCN gas. 5 mL of the sputtered ionic liquid was stirred with 5 mL of the prepared cyanide solution for 24 h.

Results and discussion

Nanoparticle growth

Gold nanoparticles were chosen as the model system as they are known to be inert to oxidation in contrast to, *e.g.*, copper nanoparticles and have been studied in a broad range of media and synthesized by various techniques.[21,22] Gold nanoparticles were synthesized by sputter deposition on an ionic liquid. After sputtering, the sample was homogenized by stirring with a small glass rod or by shaking the solution manually. Sonication was found to destabilize the nanoparticle suspension and induce aggregation. The samples were kept in a closed quartz cuvette and stored in a dessicator or glove-box (<2 ppm H_2O) to keep the samples dry. The color of the ionic liquid changed from colorless to brown during the sputtering experiment. To verify whether the color change was due to the sputtered gold (atoms/clusters/nanoparticles) or to a partial decomposition of the ionic liquid a gold extraction of the sputtered ionic liquid suspension with an aqueous solution of sodium cyanide (10^{-1} M) was performed:

$$4Au + 8NaCN + O_2 + 2H_2O \rightarrow 4NaAu(CN)_2 + 4NaOH$$

The color of the sputtered sol changed from brown to colorless or slightly yellow (*i.e.* the color of the pure ionic liquid before sputtering) during the extraction. This shows that the brown color after sputtering stems from the gold inside the ionic liquid and is not due to decomposition of the ionic liquid during the sputtering process. To exclude that hydrolysis of impurities, which might be responsible for the coloring of the

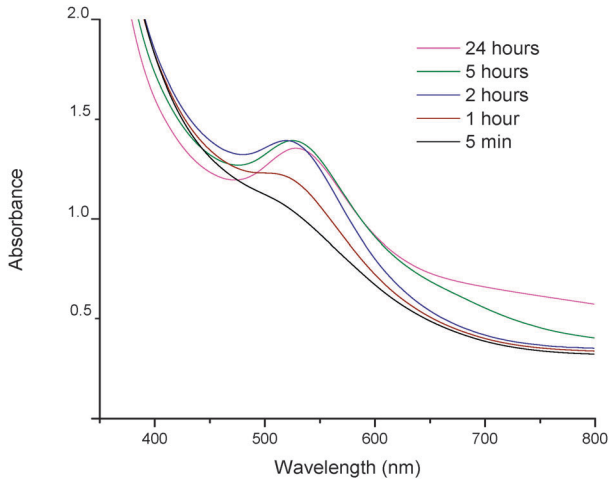

Fig. 1 UV-VIS absorption spectra of gold nanoparticles dispersed in the ionic liquid $[C_1C_4Im][N(CN)_2]$ as a function of time after sputter deposition. The spectra have been recorded at room temperature in a closed quartz cuvette.

ionic liquid, took place at this high pH value the experiment was repeated without adding NaCN to the solution. The sputtered ionic liquid did not show any decolorization when stirred with this solution.

In Fig. 1 the UV-VIS absorption spectra of a sample of the $[C_1C_4Im][N(CN)_2]$ ionic liquid with gold sputtered on it are shown at different time intervals. Immediately after sputtering no surface plasmon resonance (SPR) band was observed. Gradually a shoulder started to form and after 2 hours a well-developed surface plasmon resonance band was present around 520 nm. The appearance of an SPR band is typical for gold nanoparticles with sizes to a few hundred nm and is responsible for the characteristic red color of a sol of gold NPs.[9] It is also known that this plasmon resonance band is absent for very small NPs (<2.5 nm in diameter).[13] The color of this $[C_1C_4Im][N(CN)_2]$ sample changed from brown to red in the first two hours after sputtering. Samples of the gold nanoparticles were also analyzed by TEM. These samples were taken from the bulk ionic liquid at the same time intervals as those used for the absorption spectra. In the sample taken 1 minute after the end of the sputtering process, only very small nanoparticles in the range from 1 to 2.5 nm could be observed (Fig. 2a). There are possibly even smaller nanoparticles present, but these could not be identified with certainty in the TEM images due to the background contrast caused by the ionic liquid. These nanoparticles smaller than 2.5 nm are not expected to exhibit surface plasmon resonance and this is in agreement with the corresponding absorption spectra (Fig. 1). After 2 hours, small nanoparticles ranging from 1 to 2.5 nm were still predominantly present, but also larger nanoparticles in the range from 3 to 7 nm were formed (Fig. 2b). It is known that the driving force for smaller particles to form larger particles is their large surface tension.[12] The surface energy increases substantially as the radius decreases below 3 nm, which can be expected because the average coordination number of the surface atoms decreases.[18] A bimodal size-distribution was found to develop. These larger nanoparticles are expected to exhibit an SPR band and this corresponds with the absorption spectra in Fig. 1.[23,24] More and more larger NPs in the range from 3 to 7 nm could be observed in the TEM images as a function of time (Fig. 2a–d). It is impossible to determine the absolute concentration of the nanoparticles from TEM images, but it is clear that the ratio of larger nanoparticles to the smaller primary nanoparticles increases as a function of time. After 24 hours (Fig. 2d), the larger NPs

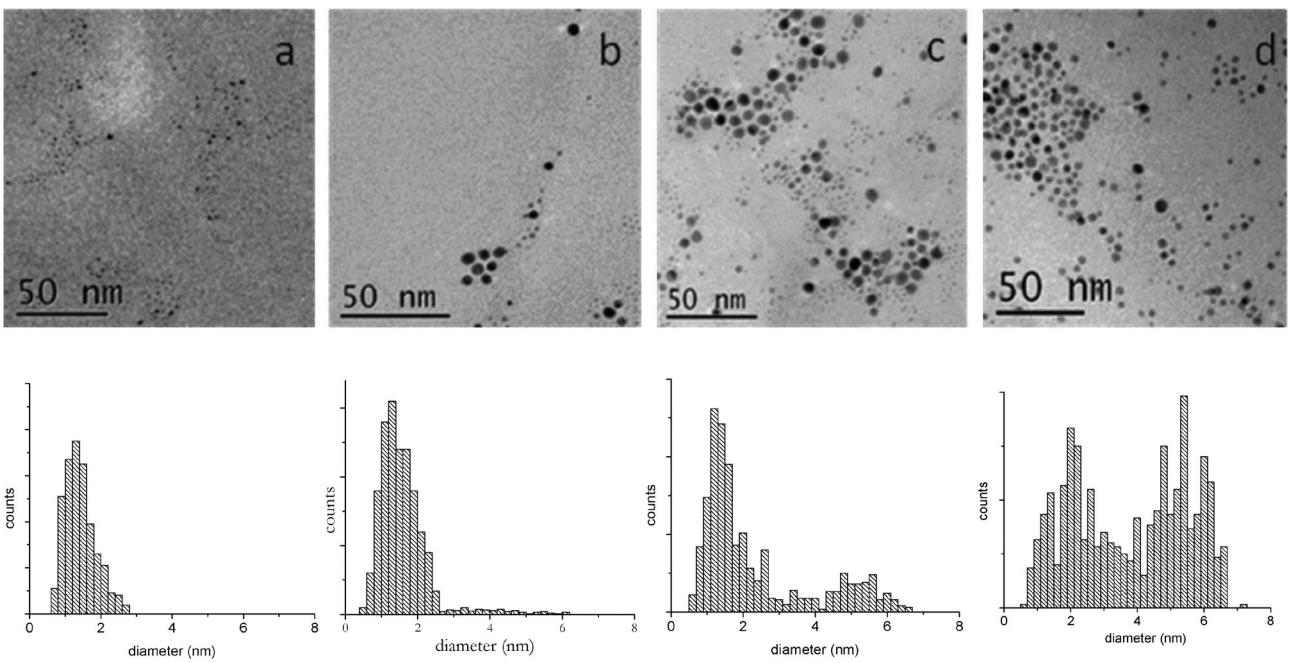

Fig. 2 Representative TEM images of gold nanoparticles in the ionic liquid $[C_1C_4Im][N(CN)_2]$ sampled from the bulk ionic liquid (a) 1 minute after sputtering, (b) 2 hours after sputtering, (c) 6 hours after sputtering and (d) 24 hours after sputtering, with the corresponding histograms of the size-distribution of gold nanoparticles below.

were as abundant as the smaller nanoparticles. Even though NPs with sizes of 7 nm are already observed after 2 hours, no NPs larger than 7 nm were observed, not even after 24 hours. This means that the nanoparticles stop growing at a certain size, in this case a diameter of about 6 nm. Because after 2 hours there is plenty of gold precursor present to enable further growth of the larger NPs, the reason for this observation should be searched elsewhere. Because of the clean synthesis procedure used (*i.e.* sputtering), the only species present in these samples besides gold is the ionic liquid. The formation of a stabilizing ionic liquid layer around these larger nanoparticles could explain our observations. This is in agreement with the reports on layering of ionic liquids close to a surface and the stabilization mechanism proposed by Rubim *et al.*[10,14] In other words the ionic liquid fulfills a stabilizing function analogous to that of a capping agent in an aqueous suspension. Further investigation on this matter is necessary and will be the subject of a second paper. These results clearly show that very small primary nanoparticles (<2.5 nm) are present in the sample immediately after sputtering and that afterwards a rather slow growth process takes place in the ionic liquid producing larger NPs.

Stability of the suspensions

Water was found to have a major influence on the stability of colloidal suspensions of gold nanoparticles in ionic liquids. This confirms previous reports on this matter.[14] Although we worked in the dryest possible conditions it was noticed that after a few hours two other processes besides the growth process took place, namely aggregation and sedimentation of the gold nanoparticles. This is evident from the UV/visible absorption spectra shown in Fig. 1. The red-shift in the SPR band position indicates that larger aggregates (superstructures composed of aggregated, but not sintered NPs) are being formed or that larger NPs are being formed.[11] Since we do not observe nanoparticles larger than 7 nm we conclude that the shift is due to aggregates formed in the sol.

Influence of ionic liquid viscosity

The *in situ* growth of sputtered gold nanoparticles was also investigated in other ionic liquids: $[C_1C_4Im][Tf_2N]$, $[C_1C_4Im][BF_4]$, $[C_1C_4Im][PF_6]$ and $[C_1C_4Im][TfO]$. The nanoparticle growth in these ionic liquids is slower than in $[C_1C_4Im][N(CN)_2]$. In Fig. 3 one can observe that the development of the SPR band is proceeding at different speeds for all the tested ionic liquids. For $[C_1C_4Im][N(CN)_2]$, the SPR band is at its maximum after 4 hours, while for $[C_1C_4Im][Tf_2N]$ it takes 12 hours to reach to its maximum. For the ionic liquids $[C_1C_4Im][TfO]$, $[C_1C_4Im][BF_4]$ and $[C_1C_4Im][PF_6]$ it took more than 24 hours before the SPR absorption band reached its maximum. These observations indicate that the growth of gold nanoparticles proceeds at different speeds in different ionic liquids. As already stated by Hatakeyama *et al.*, the viscosity of the ionic liquid plays an important role in the synthesis of nanoparticles

Table 1 Viscosities of ionic liquids used in this study, measured at 25 °C

Ionic liquid	Viscosity/Pa s
$[C_1C_4Im][N(CN)_2]$	0.032
$[C_1C_4Im][Tf_2N]$	0.056
$[C_1C_4Im][TfO]$	0.075
$[C_1C_4Im][BF_4]$	0.095
$[C_1C_4Im][PF_6]$	0.354

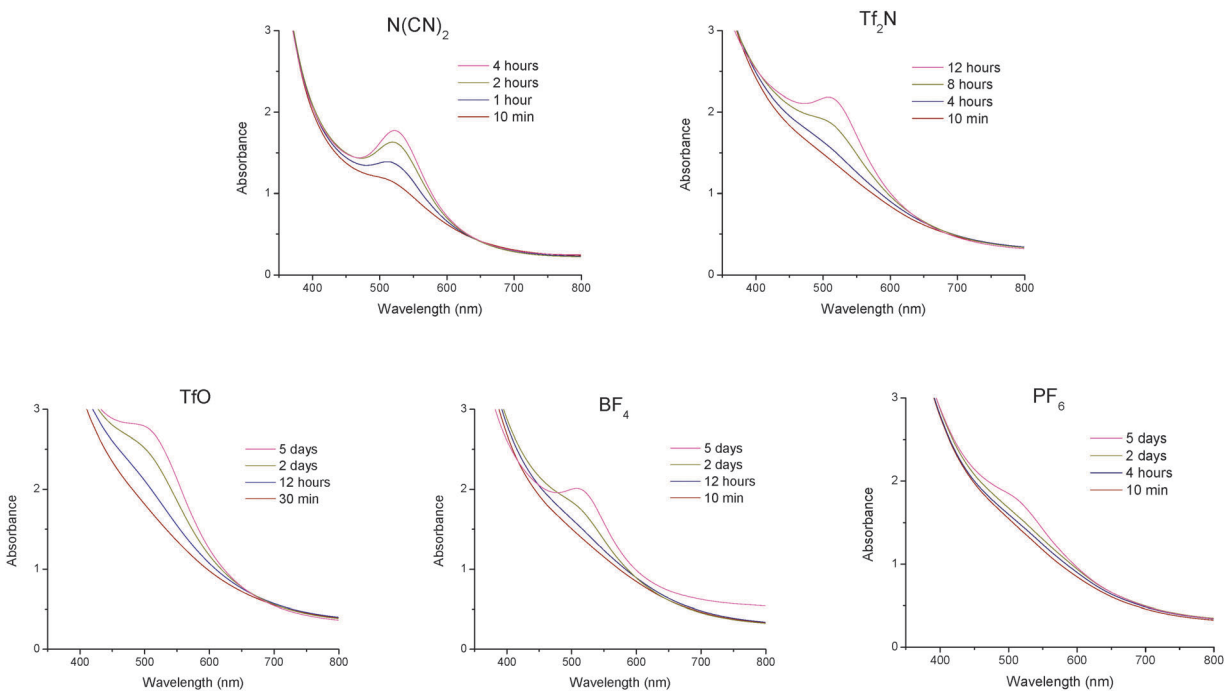

Fig. 3 UV-VIS absorption spectra of gold nanoparticles dispersed in the ionic liquids $[C_1C_4Im][N(CN)_2]$, $[C_1C_4Im][Tf_2N]$, $[C_1C_4Im][TfO]$, $[C_1C_4Im][BF_4]$ and $[C_1C_4Im][PF_6]$ as a function of time after sputter deposition. The spectra have been recorded at room temperature in a closed quartz cuvette.

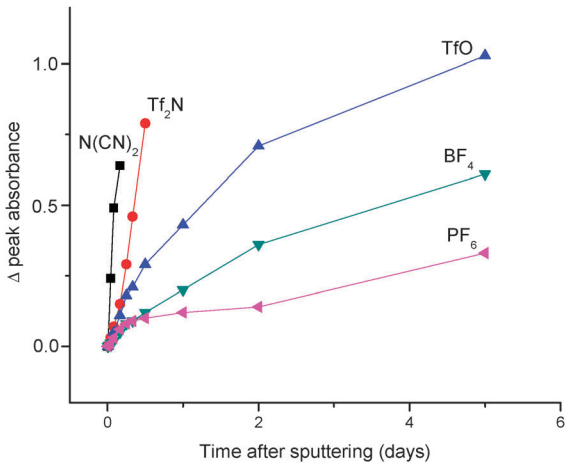

Fig. 4 Peak absorbance as a function of time after sputtering in the different ionic liquids: $[C_1C_4Im][N(CN)_2]$, $[C_1C_4Im][Tf_2N]$, $[C_1C_4Im][TfO]$, $[C_1C_4Im][BF_4]$ and $[C_1C_4Im][PF_6]$.

via sputter deposition.[7] Table 1 shows the viscosities of the ionic liquids used in this study. When comparing the absorption spectra in Fig. 3 with these viscosity values a striking trend is observed: the more viscous the ionic liquid is, the slower is the nanoparticle growth. This statement is visualized in Fig. 4 where the peak absorbance of the SPR band is plotted as a function of time after sputtering for the different ILs. Because only the larger NPs (3–7 nm) exhibit an SPR band and the initial concentration of sputtered gold is the same for all batches, we used the increase in peak absorbance, which is a function of the increase in the fraction of the larger gold NPs in the system, as a measure of the growth speed of the NPs. The peak absorbances at time 1 min are set to zero for ease of comparison. It is clear that the growth of the SPR band is fastest for $[C_1C_4Im][N(CN)_2]$ and shows the following trend: $[C_1C_4Im][N(CN)_2] > [C_1C_4Im][Tf_2N] > [C_1C_4Im][TfO] > [C_1C_4Im][BF_4] > [C_1C_4Im][PF_6]$. A growth mechanism that involves a diffusion limited growth of the nanoparticles in the ionic liquids can explain these observations. The growth rate of the gold nanoparticles is not only governed by viscosity, but other parameters such as chemical composition of the ionic liquid will also have an influence on the growth process. Aside from the growth process other processes such as flocculation and sedimentation will have an influence on the SPR absorbance, which is used as a measure for the growth rate. There is no one-to-one correlation between viscosity and growth speed, but the trend is obvious for all tested ILs: the higher the viscosity, the slower the growth rate.

These observations indicate that the gold nanoparticles grow inside the ionic liquid after the end of the sputter deposition process and that the viscosity plays an important role in the growth process as also stated by Torimoto and co-workers.[15] Hatakeyama and co-workers recently concluded that the collision frequency of the gold NPs is an important factor and is influenced by temperature and viscosity of the IL.[16]

Influence of metal concentration

According to Torimoto *et al*. the sputter time does not have a significant influence on the size and size-distribution of the gold nanoparticles.[4] Because Torimoto and co-workers did not mention an intrinsic dynamic growth process that takes place in a sputtered ionic liquid we re-investigated the influence of sputter time on the growth process. Two batches of $[C_1C_4Im][N(CN)_2]$ with a water content of <30 ppm were sputtered during 30 s and 150 s, respectively. The growth process was monitored as discussed above. To have an idea of the concentration during sputtering a thickness measurement was performed by placing a quartz crystal microbalance (QCMB) in the vacuum chamber. The thickness of the gold layers after 30 s and 150 s sputtering was 9 nm and 88 nm, respectively. These values correspond to concentrations of 40 ppm Au (40 μg gold/g IL) and 390 ppm Au (390 μg gold/g IL). TXRF analysis of these samples after the growth process revealed a gold concentration of 44 μg g^{-1} for the 30 s sample and 434 μg g^{-1} for the 150 s sample and shows good agreement with the estimated concentrations using a QCMB.

As can be seen in Fig. 5, the UV/VIS absorption spectra of the two samples show that the background absorption value for the 30 s sample is significantly lower than the absorption value for the 150 s sample which results from the higher concentration of gold nanoparticles for the latter. Notice that the absorption spectra were recorded with a quartz cuvette with a path length of 2 mm instead of 10 mm for the more concentrated sample, which decreased the absorption by a factor of 5 according to the law of Lambert–Beer. Another observation that is made from Fig. 5 is that the absorbance of the SPR band increases faster for the 150 s sample than for the 30 s sample. TEM analysis at different time intervals showed that the size distribution of the nanoparticles ranged from 1–7 nm and was in the same range as the histograms displayed in Fig. 2. The change in size-distribution is similar to those shown in Fig. 2 and follows the same trend for both samples. The difference lies in the fact that larger nanoparticles in the range of 4–6 nm appeared at earlier times and in higher abundance in the more concentrated sample. This can also be seen in the absorption spectra which show that for the more concentrated sample the SPR band already appeared after 10 minutes while for the 30 s sample the band only became apparent after a few hours. The bottom graph of Fig. 5 shows the peak absorption of the SPR band plotted as a function of time. The peak of the 150 s sample grew much faster than the peak for the 30 s sample. This indicates that the population of larger particles contributing to this SPR band grows faster for the more concentrated sample. The slope of both curves is a measure of the growth speed. It is very fast at the start of the growth process and slower when proceeding in time. The explanation can be found in the decrease in concentration of the small primary NPs (*circa* 1.5 nm), which we believe are the precursor for the larger (*circa* 5 nm) NPs. The abundance of these small NPs is the highest at the beginning of the growth process and they are consumed during the growth process. This effect is much more pronounced for the high concentration sample. After 24 hours the growth speed becomes equal for both samples. These observations lead to the conclusion that we are dealing with a diffusion-limited growth process.

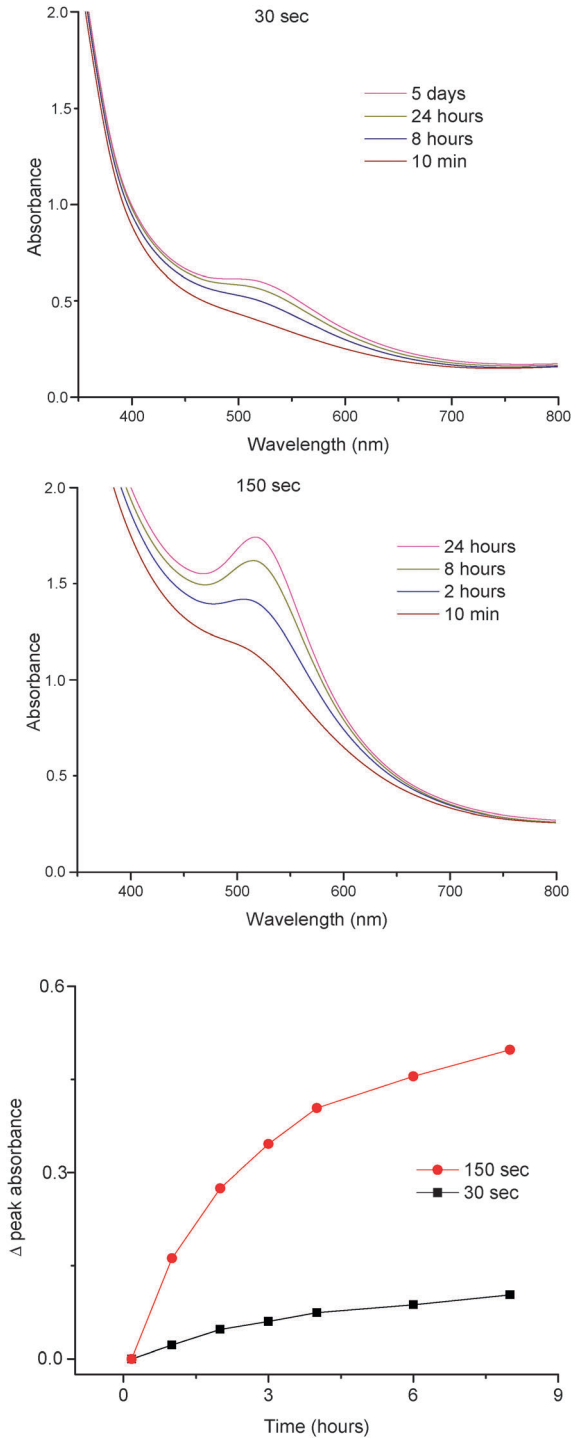

Fig. 5 UV-VIS absorption spectra of gold nanoparticles dispersed in the ionic liquid $[C_1C_4Im][Tf_2N]$ after sputtering for 30 s (top) and after 150 s (middle). The spectra have been recorded at room temperature in a closed quartz cuvette with path length 10 mm for the 30 s sample and 2 mm for the 150 s sample. The third graph (bottom) shows the evolution of the peak absorbance as a function of time.

Growth mechanism

Contrary to some authors, we are not convinced that the sputtered Au atoms that arrive at the ionic liquid interface assemble and grow into larger particles at this interface before

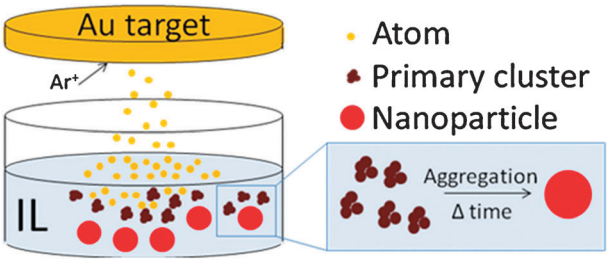

Fig. 6 Scheme of the growth mechanism of gold nanoparticles after sputter deposition onto an ionic liquid.

diffusing into the liquid.[7,19] The difference in Gibbs free energy between a spherical particle of radius a at the interface and the particle fully immersed in either of the two phases is given by:[27]

$$\Delta E = \pi a^2 \gamma (1 - \cos\theta)^2 \quad (1)$$

where a is the radius of the particle, γ the surface tension and θ the contact angle. For typical values of the surface tension of ionic liquids (40 mJ m^{-2}) and contact angles (60°), this energy difference becomes larger than 6 kT when the particle is larger than 2 nm.[28] Eqn (2) shows that the stabilisation energy of a particle increases with r^2. It is evident that if the sputtered atoms and small clusters do not immediately penetrate into the ionic liquid they will stay there and a metal film will form on the ionic liquid rather than NPs in the liquid. Hence we believe that the atoms and small clusters generated during sputtering penetrate the surface of the ionic liquid because they have sufficient kinetic energy. As a consequence nucleation and growth of the gold nanoparticles occur in the bulk phase of the IL (Fig. 6). If an evaporation method is used, films can form on the ionic liquid, because the average kinetic energy with which the atoms arrive at the ionic liquid surface is significantly lower and the flux of metal atoms is usually larger. However, even with that technique there are difficulties in obtaining a layer because of diffusion of metal NPs into the ionic liquid.[26]

As stated in the Introduction, the growth mechanisms of metal nanoparticles are currently poorly understood. A variety of nanoparticles growth mechanisms have been suggested in the literature. *Ostwald ripening* where larger nanoparticles grow at the expense of smaller ones is often used to describe the growth process of particles.[20] However, for Ostwald ripening to occur, gold atoms would have to dissolve into the ionic liquid from the smaller particles and deposit on the larger particles. As the solubility of Au^0 in an ionic liquid is negligible, this mechanism can be ruled out. From the available literature the aggregative growth mechanism described by Njoki *et al.* corresponds to our observations.[17] In this mechanism small, primary nanocrystals aggregate and coalesce to produce larger nanoparticles. However, our growth curves do not exhibit a sigmoidal shape. The initial induction-like period which is associated with nucleation at the beginning of the curves is missing. This can be explained by the absence of the nucleation stage in our measurement time frame, which probably already had finished before our absorption measurements started. Our hypothesis is that aggregation is an important process in the growth of gold nanoparticles

synthesized by sputter deposition. These findings are in agreement with the results of Janiak and co-workers and those of Torimoto and co-workers, who also found evidence for aggregative growth of metal nanoparticles in ionic liquids.[8,15]

Conclusions

This study on the growth of gold nanoparticles in ionic liquids after sputter deposition reveals a number of interesting results. Firstly it was shown that very small primary nanoparticles (<2.5 nm in diameter) are present in the sample immediately after sputtering. Secondly, after the sputter process a rather slow growth process takes place in the bulk ionic liquid. It is clear that the increase of the SPR band absorption is the fastest for the ionic liquid $[C_1C_4Im][N(CN)_2]$ batch and shows the following trend: $[C_1C_4Im][N(CN)_2]$ > $[C_1C_4Im][TfO]$ > $[C_1C_4Im][Tf_2N]$ > $[C_1C_4Im][BF_4]$ > $[C_1C_4Im][PF_6]$. A growth mechanism that involves a diffusion-limited growth of the nanoparticles in the ionic liquids can explain this observation. Thirdly, nanoparticles stop growing at a certain size, in our experiments at a diameter of about 6 nm. The formation of a stabilising ionic liquid layer around the larger nanoparticles could explain this observation. Fourthly, the population of larger particles contributing to this SPR band grows faster for the more concentrated sample. The growth speed is very fast at the start of the growth process and slows down when proceeding in time. These observations lead to the conclusion that the concentration of the gold NP precursors, which we believe are the small primary NPs, decreases over time. Fifthly, experimental observations lead to the conclusion that we are dealing with an aggregative growth process. Finally, we reasoned that NPs grow inside the ionic liquid, in contrast to previous statements that the NPs grow and nucleate on the surface of the ionic liquid.

Due to their relatively high viscosities, ionic liquids exhibit very slow diffusion kinetics compared to water and organic solvents. When synthesizing metal nanoparticles through a sputter deposition technique one should bear in mind that the growth process is very slow and can last for several hours to days. If these slow kinetics are ignored, wrong interpretations might be made when analyzing the NPs sizes and size-distributions. Not only different sputter parameters (gas pressure, current, time) used in different studies, as correctly stated by Dupont and co-workers,[19] but also the time of analysis after synthesis should be clearly stated and will make comparison between different studies in this field possible.

Acknowledgements

The authors acknowledge financial support by the K. U. Leuven (project IDO/05/005), by the FWO-Flanders (Research Community "Ionic Liquids") and by the IWT-Flanders (SBO-project "MAPIL"). Support by IoLiTec (Heilbronn, Germany) is also acknowledged. We also thank the Flemish Hercules Stichting for its support in HER/08/25. The authors acknowledge the support of the Belgian Federal Science Policy Office through the IUAP project INANOMAT (contract P6/17).

References

1 (*a*) J. Dupont, G. S. Fonseca, A. P. Umpierre, P. F. P. Fichtner and S. R. Teixeira, *J. Am. Chem. Soc.*, 2002, **124**, 4228–4229; (*b*) P. Dash and R. W. J. Scott, *Chem. Commun.*, 2009, 812–814; (*c*) P. Migowski and J. Dupont, *Chem.–Eur. J.*, 2007, **13**, 32–39; (*d*) H. Itoh, K. Naka and Y. Chujo, *J. Am. Chem. Soc.*, 2004, **126**, 3026–3027; (*e*) H. J. Ryu, L. Sanchez, H. A. Keul, A. Raj and M. R. Bockstaller, *Angew. Chem., Int. Ed.*, 2008, **47**, 7639–7643; (*f*) T. Y. Kim, W. J. Kim, S. H. Hong, J. E. Kim and K. S. Suh, *Angew. Chem., Int. Ed.*, 2009, **48**, 3806–3809; (*g*) K. Richter, A. Birkner and A. V. Mudring, *Angew. Chem., Int. Ed.*, 2010, **49**, 2431–2435; (*h*) K. Richter, A. Birkner and A. V. Mudring, *Phys. Chem. Chem. Phys.*, 2011, **13**, 7136–7141.
2 (*a*) S. A. Meiss, M. Rohnke, L. Kienle, S. Z. El Abedin, F. Endres and J. Janek, *ChemPhysChem*, 2007, **8**, 50–53; (*b*) S. Z. El Abedin, M. Polleth, S. A. Meiss, J. Janek and F. Endres, *Green Chem.*, 2007, **9**, 549–553.
3 A. Imanishi, M. Tamura and S. Kuwabata, *Chem. Commun.*, 2009, 1775–1777.
4 T. Torimoto, K. Okazaki, T. Kiyama, K. Hirahara, N. Tanaka and S. Kuwabata, *Appl. Phys. Lett.*, 2006, **89**, 243117.
5 T. Torimoto, K. Okazaki, T. Kiyama, K. Hirahara, N. Tanaka and S. Kuwabata, *Chem. Commun.*, 2009, 691–693.
6 T. Suzuki, K. Okazaki, T. Kiyama, S. Kuwabata and T. Torimoto, *Electrochemistry (Tokyo, Jpn.)*, 2009, **77**, 636–638.
7 Y. Hatakeyama, M. Okamoto, T. Torimoto, S. Kuwabata and N. Nishikawa, *J. Phys. Chem. C*, 2009, **113**, 3917–3922.
8 E. Redel, M. Walter, R. Thomann, L. Hussein, M. Krüger and C. Janiak, *Chem. Commun.*, 2010, **46**, 1159–1161.
9 S. Link and M. A. El-Sayed, *J. Phys. Chem. B*, 1999, **103**, 8410–8426.
10 (*a*) M. Mezger, H. Schroder, H. Reichert, S. Schramm, J. S. Okasinski, S. Schroder, V. Honkimaki, M. Deutsch, B. M. Ocko, J. Ralston, M. Rohwerder, M. Stratmann and H. Dosch, *Science*, 2008, **322**, 424–428; (*b*) R. Atkin, S. Z. El Abedin, R. Hayes, L. H. S. Gasparotto, N. Borisenko and F. Endres, *J. Phys. Chem. C*, 2009, **113**, 13266–13272.
11 C. D. Keating, M. D. Music, M. H. Keefe and M. J. Natan, *J. Chem. Educ.*, 1999, **76**, 949–955.
12 L. J. Lewis, P. Jensen and J.-L. Barrat, *Phys. Rev. B: Condens. Matter*, 1997, **56**, 2248.
13 U. Kreibig and M. Vollmer, Optical properties of metal clusters, Springer-Verlag, Berlin, .
14 J. C. Rubim, F. A. Trindade, M. A. Gelesky, R. F. Aroca and J. Dupont, *J. Phys. Chem. C*, 2008, **112**, 19670–19675.
15 S. Kuwabata, T. Tsuda and T. Torimoto, *J. Phys. Chem. Lett.*, 2010, **1**, 3177–3188.
16 Y. Hatakeyama, S. Takahashi and K. Nishikawa, *J. Phys. Chem. C*, 2010, **114**, 11098–11102.
17 P. N. Njoki, J. Luo, M. M. Kamundi, S. Lim and C.-J. Zhong, *Langmuir*, 2010, **26**, 13622–13629.
18 C. T. Campbell, S. C. Parker and D. E. Starr, *Science*, 2002, **298**, 811.
19 H. Wender, L. F. Oliveira, P. Migowski, A. F. Feil, E. Lissner, M. H. G. Prechtl, S. R. Teixeira and J. Dupont, *J. Phys. Chem. C*, 2010, **114**, 11764–11768.
20 W. Ostwald, *Lehrbuch der Allgemeinen Chemie*, vol. 2, part 1, Leipzig, Germany, 1896.
21 M.-C. Daniel and D. Astruc, *Chem. Rev.*, 2004, **104**, 293–346.
22 S. J. Guo and E. K. Wang, *Anal. Chim. Acta*, 2007, **598**, 181–192.
23 M. M. Alvarez, J. T. Khoury, T. G. Schaaff, M. N. Shafigullin, I. Vezman and R. L. Whetten, *J. Phys. Chem. B*, 1997, **101**, 3706.
24 J. H. Hodak, A. Henglein and G. V. Hartland, *J. Chem. Phys.*, 2000, **112**, 5942.
25 M. Wagener and B. Günther, *J. Magn. Magn. Mater.*, 1999, **201**, 41–44.
26 E. F. Borra, O. Seddikki, R. Angel, D. Eisenstein, P. Hickson, K. R. Seddon and S. P. Worden, *Nat. Lett.*, 2007, **447**, 979–981.
27 B. P. Binks, *Curr. Opin. Colloid Interface Sci.*, 2002, **7**, 21–41.
28 W. Wang and R. W. Murray, *Anal. Chem.*, 2007, **79**, 1213–1220.